Check for updates

An oscillatory plug flow photoreactor facilitates semi-heterogeneous dual nickel/carbon nitride photocatalytic C–N couplings†

Cristian Rosso, [iD] ‡[a] Sebastian Gisbertz,[bc] Jason D. Williams, [iD] [ad]
Hannes P. L. Gemoets, [iD] [e] Wouter Debrouwer, [iD] [f]
Bartholomäus Pieber [iD] *[b] and C. Oliver Kappe [iD] *[ad]

Carbon nitride materials have emerged as an efficient and sustainable class of heterogeneous photocatalysts, particularly when paired with nickel in dual catalytic cross-coupling reactions. Performing these transformations on larger scales using a continuous process is difficult due to the problems associated with handling solids in flow. By combining an oscillatory pump with a microstructured plug flow photoreactor, a stable suspension of the photocatalyst can be maintained, circumventing clogging of the reactor channels. Through careful tuning of the oscillator properties, the residence time distribution (RTD) was optimized, whilst maintaining a stable catalyst suspension. Short residence times (20 min) were achieved using optimized conditions and the recyclability of the photocatalyst was demonstrated over 10 cycles with no loss of activity. During a stable 4.5 hour scale-out demonstration, the model substrate could be isolated on 12 g scale (90% yield, 2.67 g h⁻¹). Moreover, the method was applied for the gram scale synthesis of an intermediate of the active pharmaceutical ingredient tetracaine.

Introduction

Due to the ubiquitous presence of aryl amines in natural products and pharmaceutically-relevant compounds, C–N cross-coupling reactions have become one of the most highly utilized transformations in organic synthesis.[1] Over the past two decades, the Buchwald–Hartwig coupling has been steadily improved to efficiently access this moiety using palladium catalysis.[2] Nonetheless, interest has been renewed through the possibility to overcome the typical limitations of those procedures in terms of sustainability, cost (of both metal and ligand) and harsh conditions.[3] Nickel is an appealing alternative to palladium due to its abundancy,[4] yet

must be merged with electro- or photocatalysis,[5–7] due to the inability of Ni(II) to undergo reductive elimination, unless strong bases and complex ligands are used.[8]

As recently demonstrated, dual nickel/photo catalytic cross-coupling methods represent a promising alternative to palladium catalyzed methods. However, such metallaphotoredox catalysis methodologies usually require UV irradiation or precious metal-based photoredox catalysts to turn over the nickel catalyst,[5b–d,6,9] while the use of organic photocatalysts is sometimes limited due to photobleaching.[10] Heterogeneous semiconductors, on the contrary, are stable, noble-metal free, and easy to prepare.[11] Among all heterogeneous photocatalysts, including cadmium-based semiconductors,[5g–d] carbon nitride materials (CNs) hold tremendous promise.[12]

These organic semiconductors are stable, non-toxic, and capable of promoting, amongst other transformations, a series of cross-coupling reactions in the presence of nickel.[13] Recently, mesoporous graphitic carbon nitride (mpg-CN) was shown to efficiently catalyze C–N cross couplings when irradiated with blue light.[12c] A similar protocol used a carbon nitride derivative, synthesized by co-condensation of urea and oxamide, followed by post-calcination in a molten salt (CN-OA-m).[5i] Interestingly, this catalytic system was able to convert both electron-rich and electron-poor aryl halides using blue or green light irradiation, avoiding catalyst deactivation *via* the formation of nickel-black. The CN-OA-m

[a] *Institute of Chemistry, University of Graz, NAWI Graz, Heinrichstrasse 28, 8010 Graz, Austria. E-mail: oliver.kappe@uni-graz.at*
[b] *Department of Biomolecular Systems, Max-Planck-Institute of Colloids and Interfaces, Am Mühlenberg 1, 14476 Potsdam, Germany.
E-mail: Bartholomaeus.Pieber@mpikg.mpg.de*
[c] *Department of Chemistry and Biochemistry, Freie Universität Berlin, Arnimallee 22, 14195 Berlin, Germany*
[d] *Center for Continuous Flow Synthesis and Processing (CCFLOW), Research Center Pharmaceutical Engineering GmbH (RCPE), Inffeldgasse 13, 8010 Graz, Austria*
[e] *Creaflow BVBA, Industrielaan 12, 9800 Deinze, Belgium*
[f] *Ecosynth NV, Industrielaan 12, 9800 Deinze, Belgium*
† Electronic supplementary information (ESI) available: Full experimental details, reaction setup and product characterization. See DOI: 10.1039/d0re00036a
‡ Present address: Department of Chemical and Pharmaceutical Sciences, University of Trieste, Via Licio Giorgieri 1, 34127 Trieste, Italy.

This journal is © The Royal Society of Chemistry 2020

React. Chem. Eng., 2020, 5, 597–604 | 597

photocatalyst could be recycled multiple times without any loss of its catalytic activity. The straightforward recycling strategies (centrifugation or filtration) of the carbon nitrides make them attractive for cost-efficient and sustainable processes.[11]

Photochemical transformations are generally difficult to scale-up in batch reactors as light penetration is limited (as described by the Beer–Lambert law).[14] Continuous flow photochemistry can address these drawbacks by maintaining a short irradiated path length, which also significantly improves the efficiency of photochemical reactions, leading to shorter reaction times and higher productivity.[15]

The use of solid compounds, such as CN photocatalysts, in a flow setup remains one of the central challenges in continuous processing.[16] Indeed, complex reactor designs (agitated cells or multijet oscillating disk) or continuous stirred-tank reactor (CSTR) cascades have been proposed as solutions, but maintain their intrinsic limitations of complex moving parts or poor residence time distributions.[17] Another alternative is the use of a pulsator that prevents settling of solid materials, without having issues surrounding the long term wear of moving reactor parts. This principle has been demonstrated in baffled and baffle-less tubular flow reactors for several applications (*e.g.* crystallizations, precipitations[18] and few examples of synthetic transformations).[19] However, to our knowledge, no successful efforts have been reported utilizing an oscillatory microstructured plug flow photoreactor to enable continuous heterogeneous catalysis.

Herein we report a strategy for handling solids in flow for heterogeneous photocatalysis, by using a microstructured plug flow photoreactor in combination with pulsation delivered by an pulsator. The oscillation, combined with narrow channels formed by static mixing elements in the reactor, is designed to maintain a homogenized suspension of the carbon nitride particles, mitigating the risk of settling and reactor wall fouling, regardless of the net flow rate. The feasibility of this technology was evaluated for a nickel/photo catalytic aryl amination using CN-OA-m under visible light irradiation (Fig. 1).

Results and discussion

Reaction setup and preliminary experiments

A commercially available plug flow photoreactor (HANU™ reactor, Creaflow) was employed in this study.[20] It is comprised of a Hastelloy baseplate housing a flow channel with a series of cubic static mixing elements, topped with lid and glass or quartz window to allow visible/UV light irradiation (15 mL internal volume, 2 × 2 mm channel depth and width). A symmetrical pulse was delivered by an oscillatory diaphragm pulsator unit, positioned between the reactor and a metering pump (which generates the net flow through the system). The static mixing elements split and recombine the process stream under the imposed pulsation. The narrow channels increase pulsation velocity and improve turbulence inside the reactor, encouraging suspension of
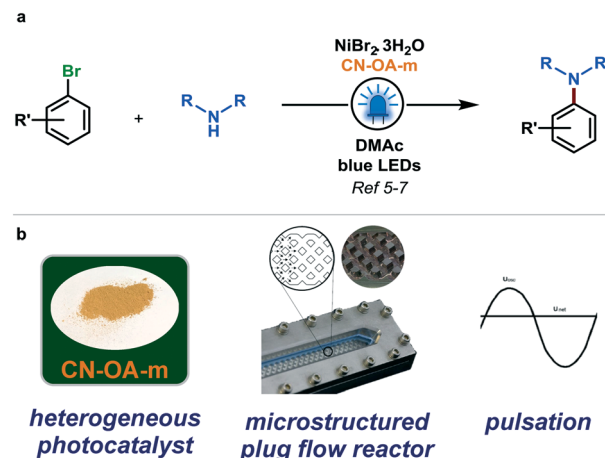

Fig. 1 (a) General scheme for the metallaphotoredox aryl amination reaction catalyzed by nickel/CN-OA-m catalysis under visible light irradiation. (b) The visual aspect of CN-OA-m photocatalyst and concept representation of the reactor in combination with an external pulsation.

solids, even at low net flow rates. In addition, the excellent film refreshment promotes efficient photon utilization for photochemical transformations. The flow reactor is equipped with an integrated heat exchanger which enables temperature control (heating or cooling) to ensure isothermal conditions.

In a typical reaction, the heterogeneous reaction mixture was kept suspended in a stirred feed vessel and fed into the system through the peristaltic metering pump, under the appropriate pulsation regime. The arrangement was pressurized at 3 bar using a back pressure regulator (BPR) capable of handling solids (BPR-10, Zaiput) and a pulsation dampener (air-filled tube connected by a Y-piece) was placed between the reactor and the BPR, in order to prevent cavitation or suction of air from the end of the system during the backward pulsation (Fig. 2).

The amination of ethyl 4-bromobenzoate (**1**) with pyrrolidine (**2a**, 3 equiv.) under blue light irradiation was selected as a model reaction. Initial reaction conditions were adapted from a previous publication: nickel(II) bromide trihydrate (2.5 mol%) and CN-OA-m (3.33 mg mL^{-1}) as metal and photocatalyst, respectively, in *N,N*-dimethylacetamide (DMAc, [**1**] = 0.2 M) (Fig. 3a).[5i] In a preliminary experiment, the pulsation amplitude was set to 70% (~0.32 mL per stroke) and the pulsation frequency to 3 Hz (100%) (see ESI† for details). By using the specified pulsation, the solid/liquid
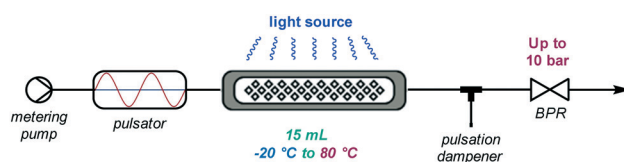

Fig. 2 Schematic representation of the reaction setup including metering pump, pulsator, reaction plate, light source, pulsation dampener and BPR. For a photograph of the setup see the ESI† Fig. S1 and S10.
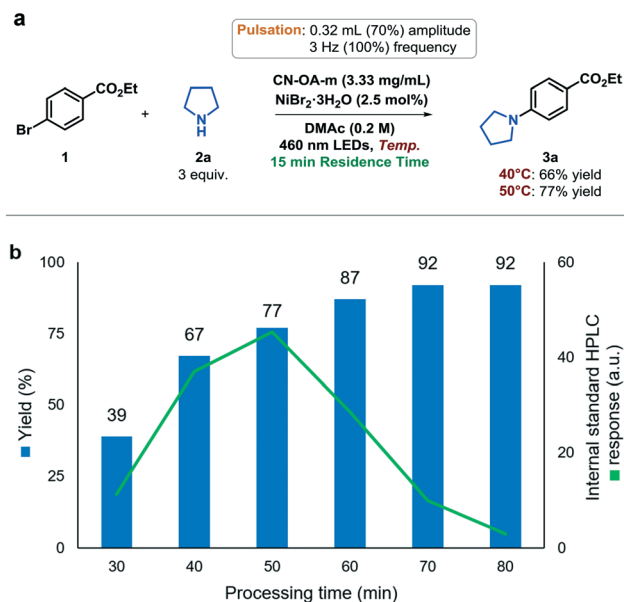
Fig. 3 (a) Reaction scheme for preliminary photochemical aryl amination experiments. Yields were determined by HPLC assay at the maximum concentration (50 min) using 4-ethylbiphenyl as the internal standard. (b) HPLC response of internal standard, relative to concentration (green line) and yield (blue bars) profile over the collection time, determined by HPLC using 4-ethylbiphenyl as the internal standard.

suspension was observed to be stable along the whole system. Gratifyingly, the C–N coupling product **3a** was observed by HPLC in 66% and 77% assay yield at 40 and 50 °C respectively using a residence time of 15 min.

The material exiting the reactor was monitored over time by HPLC, providing both its relative concentration at the analyzed time point (Fig. 3b, green line) and the assay yield of desired product **3a** (Fig. 3b, blue bars). Surprisingly, an unusual concentration/yield course was observed during these first trials. An ideal distribution of the two parameters over the time should follow a Gaussian-type profile, where the highest concentration corresponds to the highest yield.[5i,15a,21] Conversely, the observed trend showed an increasing yield after the maximum concentration was reached – a strong deviation from the expected trend. The very same concentration/yield profile was also observed in the absence of any insoluble component, suggesting that this effect is not due to the solid photocatalyst (see ESI† section B1).

To ascertain that this is phenomenon is unrelated to issues in reaching steady state conditions, the reaction was carried out with a 50 mL stock solution (in place of 25 mL), in which case an identical trend in yield was observed. Furthermore, no difference was seen when the reactor was filled with the reaction mixture prior to turning on the lamps (ensuring a constant concentration of reaction mixture at the beginning of the reaction, see ESI† section B1). A similar observation (with opposite effect) has been made in a recent report on handling solids in a photo CSTR cascade, which was explained by a poor residence time distribution.[17h]

As further validation, an experiment without photocatalyst (background reaction only) was performed both in this reactor and in a smaller plate-based photoreactor (Lab Photo Reactor, Corning).[22] In the smaller volume reactor, the expected concentration/yield plots were observed (see ESI†), implying that this deviation is due to the reactor itself. Accordingly, further efforts were devoted to the characterization of the reactor, in order to understand and minimize this effect.

Residence time distribution studies

In order to understand the reactor performance, a series of residence time distribution (RTD) experiments were designed and carried out. Specifically, these focused on the two novel process parameters in this reactor setup: pulsation amplitude (mL displaced per pump stroke) and frequency (number of strokes per second, Hz). First, the correlation between the programmed pulsation amplitude and displaced volume was quantified, proving its linearity, with a maximum displaced volume of ~0.44 mL per stroke (see ESI,† section B3).

Subsequently, an array of RTD experiments were carried out, using a colored tracer pulse and a UV/vis cell, at different pulsation amplitudes and frequencies (see ESI† section B4). As benchmark, a curve was plotted in the absence of pulsation, which resulted in a fairly wide distribution profile (Fig. 4a yellow curve). The distribution profiles proved to be
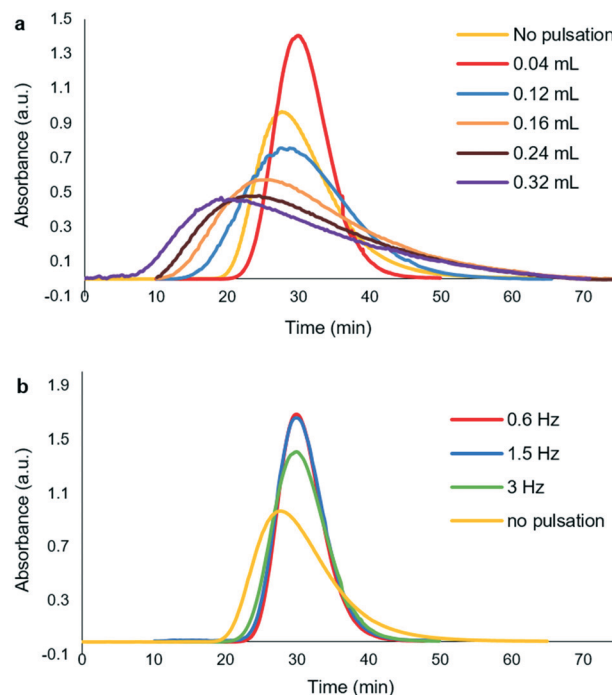

Fig. 4 RTD profiles using pulses of rose bengal dye in DMAc. Conditions: flow rate = 0.75 mL min⁻¹, back pressure = 3 bar, injected tracer volume = 1 mL. (a) Experiments performed at 3 Hz (100%) pulsation frequency and different pulsation amplitudes. (b) Experiments performed at 0.04 mL (<5%) pulsation amplitude using different pulsation frequencies.

This journal is © The Royal Society of Chemistry 2020

React. Chem. Eng., 2020, **5**, 597–604 | **599**

even broader at highpulsation amplitudes (>30% amplitude). These results could be quantified by low Bodenstein numbers (dimensionless number, Bo, which characterizes the extent of axial dispersion within the reactor), calculated from the mathematical deconvolution of the tracer experiments. The Bodenstein value should be maximized, and values below 100 represent an appreciable level of axial dispersion (*i.e.* non-ideal plug flow behavior).[23] For higher pulsation amplitudes, a decrease from 35 (at 0.12 mL amplitude) to 10 (at 0.32 mL amplitude) was observed. Gratifyingly, the lowest pulsation amplitude of 0.04 mL actually provided a significantly narrower residence time distribution curve compared to the benchmark case (without pulsation), implying a significant decrease in axial dispersion. The corresponding Bo values quantify this observation, providing a substantial increase from 48 (no pulsation) to 128 (at 0.04 mL amplitude).

The effect of pulsation frequency showed a trend of increasing Bo with decreased pulsation amplitude from 3 to 0.6 Hz (Fig. 4b). A maximum Bo value of 184 could be achieved (0.04 mL, 0.6 Hz), demonstrating plug flow behavior for the microstructured flow photoreactor. These observations serve to reinforce the significant benefits of using an oscillatory flow regime in combination with flow reactors in order to enable the handling of solids in continuous flow.

The numerical interpretation of the initial RTD (Bo = 10) trials therefore confirm the presence of a non-ideal plug flow behaviour, (see ESI† section B4). This result is consistent with the observed chemical result (Fig. 3b), since the initial reactions were performed under conditions providing an extremely low Bo value (0.32 mL, 3 Hz, Bo = 10). Based on this correlation, setting suitable pulsation parameters is essential to ensure proper suspension of the solid photocatalyst, whilst maintaining plug flow behavior (minimizing backmixing).

Optimization of the light-mediated C–N coupling

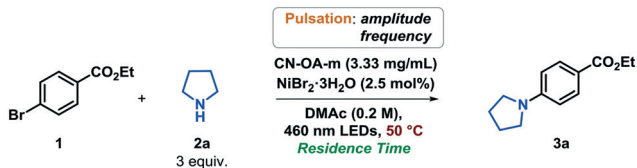In light of the preliminary results in the model aryl amination, further optimization experiments were performed minimizing the pulsation amplitude and frequency (Table 1). As anticipated, reducing the pulsation amplitude from 0.32 mL (70%) to 0.16 mL (30%) led to an increase in yield of product **3a** from 77% to 83% (entry 2, this reaction was performed in triplicate to illustrate reproducibility, see ESI† Fig. S17). In addition, lowering the amplitude to 0.12 mL (20%, the minimum value capable of keeping CN-OA-m suspended) and extending the residence time to 20 min, provided compound **3a** in 94% yield (entry 4). Finally, decreasing the pulsation frequency to the minimum affordable value of 1.5 Hz (50%) resulted in a quantitative formation of **3a** (entry 5). Furthermore, the observed yield/concentration began to follow a more expected trend, demonstrating a quasi plug flow behavior for the reaction setup (see ESI† for details). Remarkably, this demonstrates that finding the ideal compromise between sufficient solid suspension and reduced backmixing ensures excellent solid-handling and high yields of product **3a**. Compared with the previously reported procedure in batch, this flow procedure offers a significant improvement in terms of reaction time (20 minutes *vs.* 8 hours).[5i]

Photocatalyst recyclability

Likely the most substantial benefits of using a heterogeneous photocatalyst are its ease of separation (*i.e.* filtration) and potential recyclability.[13c,d,24] Therefore, we sought to determine whether the CN-OA-m catalyst is recyclable in this setup under the optimized reaction conditions. Previous studies have shown that the deposition of nickel-black agglomerates, formed over time, on the heterogeneous material can affect its catalytic properties.[5i] We envisage that, due to the far shorter irradiation time in flow, it may be possible to limit the nickel catalyst deactivation, allowing more effective recycling of the heterogeneous photocatalyst.

The CN-OA-m was recovered after each run by centrifugation, was washed, and used again in the next run by adding fresh nickel(II) bromide. Gratifyingly, no loss of activity was observed over six cycles (Fig. 5). Thereafter, a

---

Table 1 Metallaphotoredox aryl amination optimization study[a]

Pulsation: *amplitude frequency*

CN-OA-m (3.33 mg/mL)
NiBr$_2$·3H$_2$O (2.5 mol%)
DMAc (0.2 M),
460 nm LEDs, **50 °C**
Residence Time

Entry	Residence time (min)	Pulsation amplitude (mL/%)	Pulsation frequency (Hz/%)	Yield[b] (%)
1	15	0.32/70	3/100	77
2	15	0.16/30	3/100	83
3	15	0.12/20	3/100	86
4	20	0.12/20	3/100	94
5	20	0.12/20	1.5/50	99

[a] Reaction conditions: ethyl 4-bromobenzoate (**1**, 5 mmol scale), pyrrolidine (**2a**, 3 equiv.), NiBr$_2$·3H$_2$O (2.5 mol%) and CN-OA-m (3.33 mg mL^{-1}) in DMAc (0.2 M) under blue light irradiation (460 nm). Reactions were performed using a 25 mL stock solution. [b] Yield was determined by HPLC assay at the time point where concentration was at a maximum, using 4-ethylbiphenyl as the internal standard.

600 | *React. Chem. Eng.*, 2020, **5**, 597–604

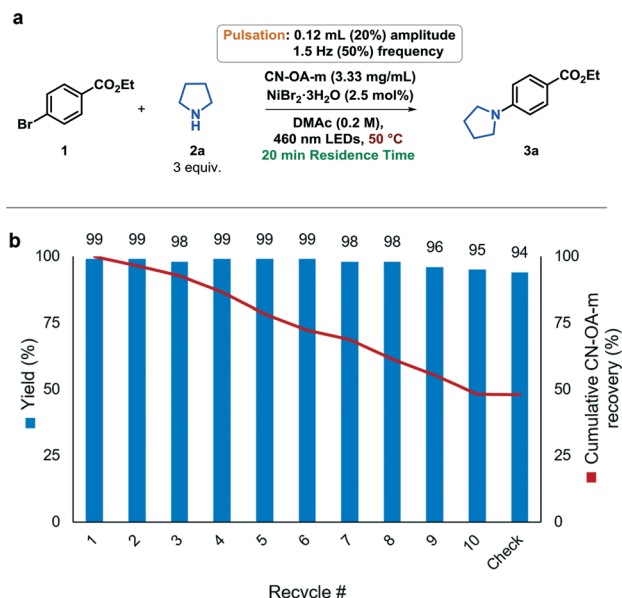This journal is © The Royal Society of Chemistry 2020

Fig. 5 (a) Reaction scheme for the CN-OA-m recycling experiments under the optimized conditions. (b) Catalytic performance of recovered CN-OA-m over ten cycles. Yield of product **3** (green bars) were determined by HPLC assay using 4-ethylbiphenyl as the internal standard at the concentration maximum over the collection time. CN-OA-m recovery (red line) was determined by weighing the recovered material after centrifugation, washing and drying.

minor reduction in the yield of **3a** was observed (from 99% to 95% yield in the tenth cycle), but this can be rationalized by the loss of small amounts of CN-OA-m (~3 mg per experiment) during the manual recovery operations between experiments. Indeed, by using fresh CN-OA-m in the same quantity as the last cycle, a comparable result was obtained
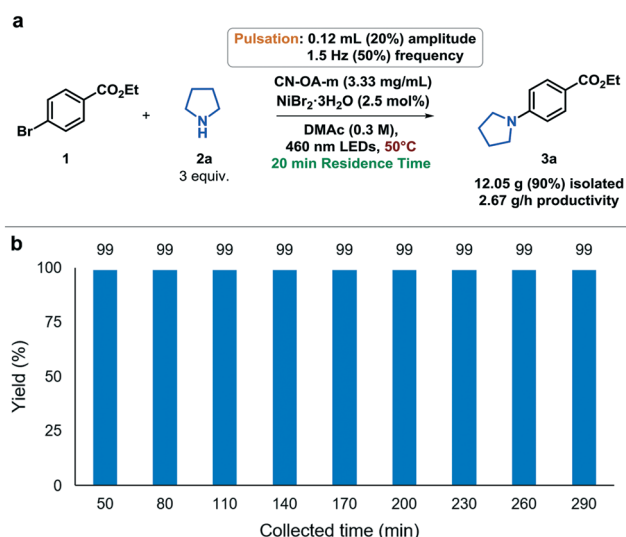

Fig. 6 (a) Reaction scheme for the CN-OA-m long run experiment under the optimized conditions, with its yield and productivity. (b) Yield of product **3** at 30 minute time increments throughout the scale out synthesis. These were determined by HPLC assay using 4-ethylbiphenyl as the internal standard.

(94% yield) confirming our hypothesis. This outcome suggests that catalyst deactivation can be avoided by using intensified conditions to prevent deleterious off-cycle side reactions.

Scale-out synthesis

A scale-out experiment was performed in order to demonstrate the stability, robustness and scalability of our protocol. It should be noted that the preparation of the CN-OA-m photocatalyst by simple calcination,[5i,13c,d] results in particles that differ in size and aggregation tendency.[25] The material was observed to have two distinct median particle sizes (D50), of ~5 μm and ~20 μm. The larger type of these particles led to a further complication in handling for long periods, due to settling in the outlet tube of the reactor, even at adequately high pulsation (see ESI† section E). Attempts to mill the particles to smaller sizes were unsuccessful.

In order to avoid this problem, the reaction setup was altered in a manner such that the reaction pathway was continually descending from the metering pump to the collection vessel (see ESI† Fig. S10). Moreover, a vibrating motor was installed on the pump inlet and every 15 minutes a small argon bubble was introduced into the system from the headspace of the starting mixture vessel. Using these modifications, the model reaction was carried out in a stable manner for over 5 hours, using the previously optimized conditions, but with a higher concentration (0.3 M instead of 0.2 M), without changing the CN-OA-m loading).
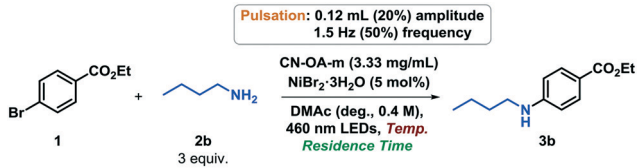
HPLC analysis revealed a stable assay yield of >99% for the duration of the experiment (Fig. 6b). The output material was collected for 4.5 hours of steady state operation, resulting in 12.05 g (90% isolated yield) of the desired coupling product **3a**, without column chromatography. This corresponds to an exceptionally high productivity of 2.67 g h^{−1} (15 mmol h^{−1}), a value to our knowledge only surpassed by some homogeneous Ir- or Ru-based photoredox catalyzed C–N couplings.[6,26] It is noteworthy that the larger version of the HANU™ reactor (150 mL volume, 10× scale up) maintains all of its process characteristics (e.g. channel dimensions, mass-, heat-, and light transfer capacities, RTD), thus allows for straightforward scale-up of such procedures.[20]
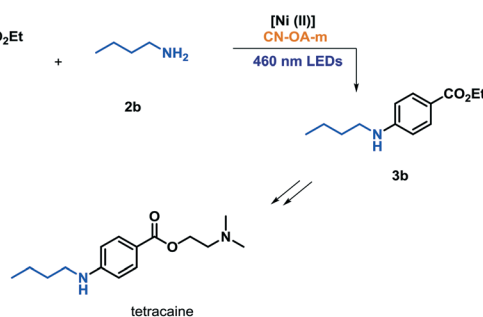
Scheme 1 Reaction scheme for the preparation of tetracaine through a photochemical aryl amination.

This journal is © The Royal Society of Chemistry 2020

React. Chem. Eng., 2020, 5, 597–604 | 601

Table 2 Tetracaine precursor optimization study[a]

Entry	Residence time (min)	Temperature (°C)	Conc (M)	NiBr$_2$·3H$_2$O (mol%)	Yield[b] (%)
1	20	60	0.2	2.5	24
2	20	60	0.4	5	38
3	60	60	0.4	5	69
4	60	80	0.4	5	94

[a] Reaction conditions: ethyl 4-bromobenzoate (**1**, 5–10 mmol scale), butylamine (**2b**, 3 equiv.), NiBr$_2$·3H$_2$O (2.5–5 mol%) and CN-OA-m (3.33 mg mL^{-1}) in DMAc (0.2–0.4 M) under blue light irradiation (460 nm). Reactions were performed using a 25 mL stock solution and 20 or 60 min residence time (0.75 or 0.25 mL min^{-1}). [b] Yield was determined by HPLC using 4-ethylbiphenyl as the internal standard.

Tetracaine precursor synthesis

Finally, we envisaged that this protocol could be used for the preparation of an active pharmaceutical ingredient (API) precursor. In particular, tetracaine,[27] a local anaesthetic selected by the World Health Organization (WHO) as an essential medicine,[28] contains a butylamino aryl core, which can be accessed from precursor **3b** by a coupling reaction between **1** and butylamine **2b** (Scheme 1). The final API can then be obtained from **3b** by simple transesterification with *N,N*-dimethylamino ethanol.[29]

Despite the use of reactive aryl bromide **1**, the coupling reaction with primary aliphatic amines is challenging and requires harsher conditions. In fact, this difference in reactivity is so substantial that recent studies have been published with the specific aim to improve their reactivity.[5c,f] An optimization study was performed starting from the previous conditions with optimized oscillation settings (Table 2). Using the previously optimized conditions, but with a slightly elevated temperature of 60 °C, product **3b** was observed in only 24% yield (entry 1). Then, increasing the concentration to 0.4 M and the nickel loading to 5 mol%, without varying the photocatalyst amount, led to a reasonable increment in yield of **3b** to 38% (entry 2). An extended residence time of 60 minutes subsequently resulted in 69% yield (entry 3). Finally, further increasing the temperature to 80 °C led to the formation of **3b** in almost quantitative yield (94%, entry 4).

It is noteworthy that under these harsh reaction conditions, the formation of a small amount of nickel-black agglomerate was observed. Notwithstanding, the result obtained is of relevance for the preparation of the API precursor, since it can be produced in a significantly shorter reaction time, when compared with the state of the art.[5c,9] Consequently, in order to isolate product **3b**, the amination reaction was carried out over a runtime of more than four hours employing the optimized conditions. The coupled product **3b** was collected in the steady state for 80 minutes (92% average HPLC assay yield), leading to an isolated yield of 1.49 g (84%), which corresponds to a productivity of 1.12 g h^{-1} (see ESI† section D2).

Conclusions

We demonstrated the utility of an oscillatory plug flow photoreactor, capable of handling solids in continuous flow for an industrially relevant metallaphotoredox C–N coupling reaction. A thorough investigation of the system performance in terms of RTD led to finding the ideal match toward processability of solids and reactor performance. Following an optimization study, excellent yield was achieved in a model C–N coupling reaction on multi-gram scale, using a short residence time. A gram-scale operation of several hours runtime demonstrated the ability to successfully scale heterogeneous photocatalysis processes by the implementation of oscillatory flow reactor technology. The intensified conditions achieved using the flow photoreactor allowed for facile recycling of the carbon nitride photocatalyst over ten cycles. Finally, a pharmaceutically relevant intermediate was synthesized using slightly modified conditions, showing its applicability for preparative scale production of medicinally relevant compounds.

Conflicts of interest

There are no conflicts to declare.

Acknowledgements

602 | *React. Chem. Eng.*, 2020, **5**, 597–604

This journal is © The Royal Society of Chemistry 2020

Notes and references

1 J. Bariwal and E. Van Der Eycken, *Chem. Soc. Rev.*, 2013, **42**, 9283–9303.

2 (*a*) R. Dorel, C. P. Grugel and A. M. Haydl, *Angew. Chem., Int. Ed.*, 2019, **58**, 17118–17129; (*b*) P. Ruiz-Castillo and S. L. Buchwald, *Chem. Rev.*, 2016, **116**, 12564–12649.

3 M. Butters, D. Catterick, A. Craig, A. Curzons, D. Dale, A. Gillmore, S. P. Green, I. Marziano, J. P. Sherlock and W. White, *Chem. Rev.*, 2006, **106**, 3002–3027.

4 J. P. Wolfe and S. L. Buchwald, *J. Am. Chem. Soc.*, 1997, **119**, 6054–6058.

5 (*a*) C. Li, Y. Kawamata, H. Nakamura, J. C. Vantourout, Z. Liu, Q. Hou, D. Bao, J. T. Starr, J. Chen, M. Yan and P. S. Baran, *Angew. Chem., Int. Ed.*, 2017, **56**, 13088–13093; (*b*) Y. Kawamata, J. C. Vantourout, D. P. Hickey, P. Bai, L. Chen, Q. Hou, W. Qiao, K. Barman, M. A. Edwards, A. F. Garrido-Castro, J. N. Degruyter, H. Nakamura, K. Knouse, C. Qin, K. J. Clay, D. Bao, C. Li, J. T. Starr, C. Garcia-Irizarry, N. Sach, H. S. White, M. Neurock, S. D. Minteer and P. S. Baran, *J. Am. Chem. Soc.*, 2019, **141**, 6392–6402; (*c*) E. B. Corcoran, M. T. Pirnot, S. Lin, S. D. Dreher, D. A. Dirocco, I. W. Davies, S. L. Buchwald and D. W. C. Macmillan, *Science*, 2016, **353**, 279–283; (*d*) Y. Du, R. M. Pearson, C. H. Lim, S. M. Sartor, M. D. Ryan, H. Yang, N. H. Damrauer and G. M. Miyake, *Chem. – Eur. J.*, 2017, **23**, 10962–10968; (*e*) C. H. Lim, M. Kudisch, B. Liu and G. M. Miyake, *J. Am. Chem. Soc.*, 2018, **140**, 7667–7673; (*f*) M. Kudisch, C.-H. Lim, P. Thordarson and G. M. Miyake, *J. Am. Chem. Soc.*, 2019, **141**(49), 19479–19486; (*g*) J. A. Caputo, L. C. Frenette, N. Zhao, K. L. Sowers, T. D. Krauss and D. J. Weix, *J. Am. Chem. Soc.*, 2017, **139**, 4250–4253; (*h*) Y. Y. Liu, D. Liang, L. Q. Lu and W. J. Xiao, *Chem. Commun.*, 2019, **55**, 4853–4856; (*i*) S. Gisbertz, S. Reischauer and B. Pieber, ChemRxiv, 2019, DOI: 10.26434/chemrxiv.10298735.v1; (*j*) J. Twilton, C. C. Le, P. Zhang, M. H. Shaw, R. W. Evans and D. W. C. MacMillan, *Nat. Rev. Chem.*, 2017, **1**, 0052.

6 B. Y. Park, M. T. Pirnot, S. L. Buchwald, B. Y. Park, M. T. Pirnot and S. L. Buchwald, *J. Org. Chem.*, 2020, DOI: 10.1021/acs.joc.9b03107.

7 (*a*) Z. H. Qi and J. Ma, *ACS Catal.*, 2018, **8**, 1456–1463; (*b*) R. Sun, Y. Qin, S. Ruccolo, C. Schnedermann, C. Costentin and D. G. Nocera, *J. Am. Chem. Soc.*, 2019, **141**, 89–93.

8 C. M. Lavoie and M. Stradiotto, *ACS Catal.*, 2018, **8**, 7228–7250.

9 M. S. Oderinde, N. H. Jones, A. Juneau, M. Frenette, B. Aquila, S. Tentarelli, D. W. Robbins and J. W. Johannes, *Angew. Chem., Int. Ed.*, 2016, **55**, 13219–13223.

10 N. A. Romero and D. A. Nicewicz, *Chem. Rev.*, 2016, **116**, 10075–10166.

11 (*a*) D. Friedmann, A. Hakki, H. Kim, W. Choi and D. Bahnemann, *Green Chem.*, 2016, **18**, 5391–5411; (*b*) P. Riente and T. Noël, *Catal. Sci. Technol.*, 2019, **9**, 5186–5232.

12 (*a*) Y. Wang, X. Wang and M. Antonietti, *Angew. Chem., Int. Ed.*, 2012, **51**, 68–89; (*b*) A. Savateev and M. Antonietti, *ACS Catal.*, 2018, **8**, 9790–9808; (*c*) I. Ghosh, J. Khamrai, A. Savateev, N. Shlapakov, M. Antonietti and B. König, *Science*, 2019, **365**, 360–366; (*d*) Y. Markushyna, C. A. Smith and A. Savateev, *Eur. J. Org. Chem.*, 2019, 1–17.

13 (*a*) M. Antonietti, A. Savateev, I. Ghosh and B. König, *Angew. Chem., Int. Ed.*, 2018, **57**, 15936–15947; (*b*) Q. Dong, N. Mohamad Latiff, V. Mazánek, N. F. Rosli, H. L. Chia, Z. Sofer and M. Pumera, *ACS Appl. Nano Mater.*, 2018, **1**, 4442–4449; (*c*) C. Cavedon, A. Madani, P. H. Seeberger and B. Pieber, *Org. Lett.*, 2019, **21**, 5331–5334; (*d*) B. Pieber, J. A. Malik, C. Cavedon, S. Gisbertz, A. Savateev, D. Cruz, T. Heil, G. Zhang and P. H. Seeberger, *Angew. Chem., Int. Ed.*, 2019, **58**, 9575–9580.

14 D. Cambié, C. Bottecchia, N. J. W. Straathof, V. Hessel and T. Noël, *Chem. Rev.*, 2016, **116**, 10276–10341.

15 For recent reviews, see: (*a*) M. B. Plutschack, B. Pieber, K. Gilmore and P. H. Seeberger, *Chem. Rev.*, 2017, **117**, 11796–11893; (*b*) L. D. Elliott, J. P. Knowles, P. J. Koovits, K. G. Maskill, M. J. Ralph, G. Lejeune, L. J. Edwards, R. I. Robinson, I. R. Clemens, B. Cox, D. D. Pascoe, G. Koch, M. Eberle, M. B. Berry and K. I. Booker-Milburn, *Chem. – Eur. J.*, 2014, **20**, 15226–15232; (*c*) J. P. Knowles, L. D. Elliott and K. I. Booker-Milburn, *Beilstein J. Org. Chem.*, 2012, **8**, 2025–2052; (*d*) F. Politano and G. Oksdath-Mansilla, *Org. Process Res. Dev.*, 2018, **22**, 1045–1062; (*e*) T. Noël, *J. Flow Chem.*, 2017, **7**, 87–93.

16 (*a*) R. L. Hartman, *Org. Process Res. Dev.*, 2012, **16**, 870–887; (*b*) K. Wu and S. Kuhn, *Chim. Oggi*, 2014, **32**, 62–66.

17 (*a*) D. L. Browne, B. J. Deadman, R. Ashe, I. R. Baxendale and S. V. Ley, *Org. Process Res. Dev.*, 2011, **15**, 693–697; (*b*) L. Liguori and H. R. Bjørsvik, *Org. Process Res. Dev.*, 2011, **15**, 997–1009; (*c*) S. Falß, G. Tomaiuolo, A. Perazzo, P. Hodgson, P. Yaseneva, J. Zakrzewski, S. Guido, A. Lapkin, R. Woodward and R. E. Meadows, *Org. Process Res. Dev.*, 2016, **20**, 558–567; (*d*) P. Filipponi, A. Gioiello and I. R. Baxendale, *Org. Process Res. Dev.*, 2016, **20**, 371–375; (*e*) Y. Mo and K. F. Jensen, *React. Chem. Eng.*, 2016, **1**, 501–507; (*f*) M. R. Chapman, M. H. T. Kwan, G. King, K. E. Jolley, M. Hussain, S. Hussain, I. E. Salama, C. González Nino, L. A. Thompson, M. E. Bayana, A. D. Clayton, B. N. Nguyen, N. J. Turner, N. Kapur and A. J. Blacker, *Org. Process Res. Dev.*, 2017, **21**, 1294–1301; (*g*) Y. Mo, H. Lin and K. F. Jensen, *Chem. Eng. J.*, 2018, **335**, 936–944; (*h*) A. Pomberger, Y. Mo, K. Y. Nandiwale, V. L. Schultz, R. Duvadie, R. I. Robinson, E. I. Altinoglu and K. F. Jensen, *Org. Process Res. Dev.*, 2019, **23**, 2699–2706.

18 For a review, see: (*a*) T. McGlone, N. E. B. Briggs, C. A. Clark, C. J. Brown, J. Sefcik and A. J. Florence, *Org. Process Res. Dev.*, 2015, **19**, 1186–1202; For selected examples, see: (*b*) O. Okafor, A. Weilhard, J. A. Fernandes, E. Karjalainen, R.

This journal is © The Royal Society of Chemistry 2020

React. Chem. Eng., 2020, **5**, 597–604 | **603**

Goodridge and V. Sans, *React. Chem. Eng.*, 2017, **2**, 129–136; (*c*) C. González Niño, N. Kapur, M. F. King, G. de Boer, A. J. Blacker, R. Bourne and H. Thompson, *Int. J. Comut. Fluid Dyn.*, 2019, **33**, 317–331; (*d*) F. Tahir, K. Krzemieniewska-Nandwani, J. Mack, D. Lovett, H. Siddique, F. Mabbott, V. Raval, I. Houson and A. Florence, *Control Eng. Pract.*, 2017, **67**, 64–75; (*e*) C. J. Brown, T. Mcglone, S. Yerdelen, V. Srirambhatla, F. Mabbott, R. Gurung, M. L. Briuglia, B. Ahmed, H. Polyzois, J. Mcginty, F. Perciballi, D. Fysikopoulos, P. Macfhionnghaile, H. Siddique, V. Raval, T. S. Harrington, A. D. Vassileiou, M. Robertson, E. Prasad, A. Johnston, B. Johnston, A. Nordon, J. S. Srai, G. Halbert, J. H. Ter Horst, C. J. Price, C. D. Rielly, J. Sefcik and A. J. Florence, *Mol. Syst. Des. Eng.*, 2018, **3**, 518–549; (*f*) C. J. Brown, J. A. Adelakun and X.-W. Ni, *Chem. Eng. Process.*, 2015, **97**, 180–186; (*g*) H. G. Jolliffe and D. I. Gerogiorgis, *Comput. Chem. Eng.*, 2018, **118**, 224–235; (*h*) M. Jiang and X.-W. Ni, *Org. Process Res. Dev.*, 2019, **23**, 882–890; (*i*) P. Cruz, F. Rocha and A. Ferreira, *CrystEngComm*, 2016, **18**, 9113–9121.

19   B. J. Doyle, B. Gutmann, M. Bittel, T. Hubler, A. Macchi and D. M. Roberge, *Ind. Eng. Chem. Res.*, 2020, DOI: 10.1021/acs.iecr.9b04496.

20   For more information on the HANU reactor, see: http://www.creaflow.be/.

21   O. Levenspiel and K. B. Bischoff, *Ind. Eng. Chem.*, 1959, **51**, 1431–1434.

22   (*a*) C. Rosso, J. D. Williams, G. Filippini, M. Prato and C. O. Kappe, *Org. Lett.*, 2019, **21**, 5341–5345; (*b*) A. Steiner, J. D. Williams, C. Mateos and C. O. Kappe, *Green Chem.*, 2020, **22**, 448–454.

23   O. Levenspiel, *Chemical Reaction Engineering*, John Wiley & Sons, 3rd edn, 1999.

24   B. Pieber, M. Shalom, M. Antonietti, P. H. Seeberger and K. Gilmore, *Angew. Chem., Int. Ed.*, 2018, **57**, 9976–9979.

25   G. Zhang, G. Li, Z. Lan, L. Lin, A. Savateev, T. Heil, S. Zafeiratos, X. Wang and M. Antonietti, *Angew. Chem., Int. Ed.*, 2017, **56**, 13445–13449.

26   K. C. Harper, E. G. Moschetta, S. V. Bordawekar and S. J. Wittenberger, *ACS Cent. Sci.*, 2019, **5**, 109–115.

27   S. Gyorke, V. Lukyanenko and I. Gyorke, *J. Physiol.*, 1997, **500**, 297–309.

28   World Health Organization Model List of Essential Medicines - 21st List, 2019.

29   M. L. Yuan, J. H. Xie and Q. L. Zhou, *ChemCatChem*, 2016, **8**, 3036–3040.

604 | *React. Chem. Eng.*, 2020, **5**, 597–604

This journal is © The Royal Society of Chemistry 2020